Epoxy Networks Reinforced with Polyhedral Oligomeric Silsesquioxanes: Structure and Segmental Dynamics as Studied by Solid-State NMR

Jiri Brus,* Martina Urbanová, and Adam Strachota

Institute of Macromolecular Chemistry, Academy of Sciences of the Czech Republic, Heyrovsky sq. 2, 162 06 Prague 6, Czech Republic

Received September 25, 2007; Revised Manuscript Received November 12, 2007

ABSTRACT: The epoxy networks based on poly(propylene oxide) chains cross-linked by diglycidyl ether of Bisphenol A and reinforced by polyhedral oligomeric silsesquioxanes (POSS) provide a typical example of polymer nanocomposites with hierarchical architecture. In addition to characterizing the epoxy−POSS composites, this contribution demonstrates valuable applications of solid-state NMR spectroscopy. The size of domains in the nanocomposites was determined by high-speed MAS $^1H-^1H$ spin-diffusion experiments, offering an alternative to the established methods like SAXS, EM, or AFM. While the latter might fail under certain circumstances (low contrast, or small domains), the $^1H-^1H$ spin-diffusion measurement yielded the size of unbroken primary domains, making also possible their distinction from "aggregates of primary domains", the size of the latter being measured by EM or SAXS. Depending on the type of the investigated network the size of the POSS aggregates arising in the nanocomposites was determined to be ca. 1−20 nm. Investigations of molecular dynamics (various "domain-selective" relaxation and recoupling solid-state NMR experiments were applied) yielded information making possible the assignment of the contribution of molecular segments to thermomechanical properties like glass transition temperature and storage shear modulus, and to predict the products' ability to absorb mechanical energy. Remarkable motional heterogeneities were found not only in the amorphous phase, where mobile polymer segments of the "free" domains coexist with the immobilized chains of the "constrained" ones, but also in the crystallites of POSS building blocks, where the amplitudes of segmental reorientations occurring in the midkilohertz frequency region remain relatively large: two-site 180° flips dominating to aromatic rings in the $POSS_{Ph}$ crystallites are accompanied by the wobbling of the flip axes with an average fluctuation angle ca. 25°. Similarly, cyclopentyl substituents in the $POSS_{Cp}$ crystallites undergo to ca. 35° rotational-diffusion motion.

Introduction

Since the end of the last century, polymer nanocomposites have offered interesting prospects for material science due to the potential improvements in mechanical and thermal properties achieved by synergistic effects between suitably chosen nanoparticles and macromolecular matrix. Among many approaches like blending of polymers with spherical nanoparticles,[1] carbon nanotubes,[2] or layered silicates,[3] the synthesis of organic−inorganic polymer nanocomposites containing well-defined inorganic cages has gained increasing popularity.[4−9] The most common compounds used for these purposes are polyhedral oligomeric silsesquioxanes (POSS) of the type $(R-SiO_{1.5})_8$.[10] Their popularity follows from easily accessible functionalization on the organic groups R permitting their incorporation into a wide range of thermoplastics or thermosets without modification of the existing manufacturing protocols. The resulting materials then exhibit modified mechanical properties, and the ultimate effect strongly depends on the type and functionality of organic substituents of the POSS units.[4−9]

One of the current trends in macromolecular chemistry is the design of multiphase nanoheterogeneous materials with tunable properties. Besides a large synthetic effort, the achievement of this target must be supported by the deep characterization of the resulting products because correlations between chemical composition and macroscopic properties provide essential information for their optimal development. As a contribution to this trend we would like to present the results of our investigations of the recently prepared POSS-reinforced epoxy networks[11,12] consisting of poly(oxypropylene)diamine cross-linked by diglycidylether of Bisphenol A. Keeping in mind that the cause of many properties of polymer materials can be found at molecular level, we focused our attention on the analysis of the basic structural motifs and segmental dynamics. In general, only a few types of the epoxy networks can be distinguished according to the topologies of POSS building blocks, that can be found (i) as randomly incorporated pendant units, (ii) as regularly repeating substituents on the backbone, (iii) as linear linkers or network cross-links, and finally (iv) as an unbound nanofiller. In all these cases, previous X-ray diffraction measurements[11] revealed the tendency of POSS units to aggregation,[13,14] and the systematic investigation of thermomechanical properties showed that the strongest reinforcement was reached in the networks where POSS units form crystalline domains.[12] However, in these materials, one cannot expect a simple relationship between the polymer composition and material properties because many effects are operating simultaneously. That is why the disclosure of the fine relations involving all the possible contributions requires analytical techniques that are complementary to the traditional tools. Owing to the recent developments of the techniques probing interatomic proximities[15−18] and amplitudes of segmental motions,[19−21] the solid-state NMR spectroscopy became an inherent tool in the characterization of polymer nanocomposites.[22−29]

In our investigation we focused on the elucidation of the nature of the "POSS effect" via the description of the local architecture at nanometer scale and by detailed analysis of segmental dynamics. The composition and motional homogeneity of the studied POSS-reinforced epoxy systems was basically probed by simple ^{13}C and ^{29}Si MAS and CP/MAS NMR experi-

* To whom correspondence should be addressed. E-mail: brus@imc.cas.cz. Telephone: +420 296 809 380. Fax: +420 296 809 410.

10.1021/ma702140g CCC: $40.75
Published on Web 12/18/2007

Table 1. Composition of POSS−Modified Epoxy Networks and Their Thermomechanical Properties[12]

type and name of network	wt % of POSS compound	wt % of POSS units incl org "substituent shell"	T_g[a] [°C]	G' at 25 °C[b] [MPa]
networks with POSS in junctions				
POSS,E8−D2000	3	31	−45	3.8
POSS,E4−D2000	47	47	−51	1.9
network with POSS in chain backbone				
POSS,E2−D2000	64	64	−60	0.55
network with nonbonded POSS nanofiller				
POSS,E0−D2000	7	7	−36	1.1
networks with monofunctional pendent POSS				
DGEBA−$POSS_{Ph,}$E1(x=0.2)−D2000	25	25	−30	3.4
DGEBA−$POSS_{Oct,}$E1(x=0.2)−D2000	30	30	−31	0.9
networks with bifunctional pendent POSS				
DGEBA−$POSS_{DGEBA,mon}$(x=0.33)−D2000	37	27	−26	5
$POSS_{DGEBA,mon}$−D2000	68	50	−24	38
$POSS_{DGEBA,oligo}$−D2000	88	49	+20	230
reference network				
DGEBA−D2000	0	0	−29	2.0

[a] T_g [°C]: glass-transition temperature, as the temperature of the maximum of the loss factor tan δ. [b] G' [MPa]: dynamic shear storage modulus determined at 25 °C.

ments. Information about motional frequencies was obtained using various T_1 and $T_{1\rho}$ ^{13}C relaxation experiments in which the application of cross-polarization and/or direct excitation of ^{13}C spins made it possible to measure relaxation parameters selectively in rigid and mobile domains, respectively. Further, the information about motional amplitudes was obtained using "domain-selective" $^1H-^{13}C$ separated-local-field experiments.[20,21] The self-assembling of basic building units and the local geometry was probed by high-speed 2D $^1H-^1H$ MAS correlation experiments employing $^1H-^1H$ spin diffusion. Finally, the obtained structural data and the information about segmental dynamics were discussed with respect to thermomechanical properties and correlated with the observed changes in glass transition temperature (T_g) and shear storage modulus (G).

Experimental Section

Technique of Preparation of POSS-Modified Networks. The reference epoxy−amine network was prepared from diglycidyl ether of Bisphenol A (DGEBA) and poly(oxypropylene)diamine (Jeffamine D2000, molecular weight M = 2000, Huntsman Inc.). The POSS-modified epoxy networks were prepared by using epoxy-functionalized POSS monomers, $POSS_RE$*n*, obtained from Hybrid Plastics or synthesized. The POSS compounds with various number of epoxy functionalities (n = 0−8) and various organic substituents R, were employed; R = phenyl ($POSS_{Ph}$), isooctyl ($POSS_{Oct}$), or cyclopentyl ($POSS_{Cp-DGEBA}$). The synthesis of the epoxy−POSS monomers and of modified epoxy networks is described in detail in our previous papers.[11,12] The compositions and names of the hybrid networks prepared are listed in Table 1. All the systems were stoichiometric, this means that the ratio of functional groups, r = (NH/epoxy) was equal to 1.

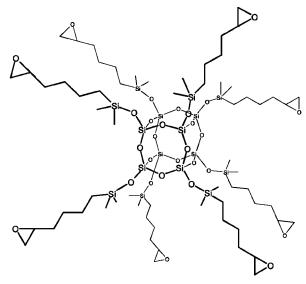

POSS,E8

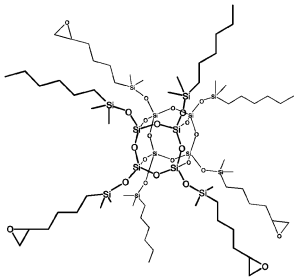

POSS,E4

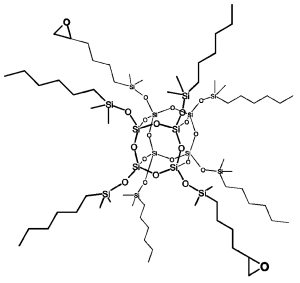

POSS,E2

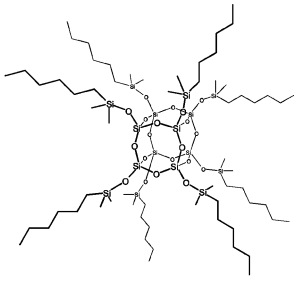

POSS,E0

Networks with POSS in Junctions. The systems belonging to this family were prepared from multifunctional epoxy−POSS monomers: octaepoxide (POSS,E8); tetraepoxide (POSS,E4) and diepoxide (POSS,E2). The epoxy groups are attached to the POSS skeleton through flexible hexyl spacers.

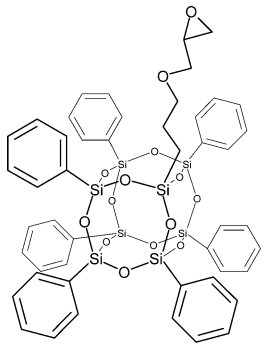

$POSS_{Ph}$E1

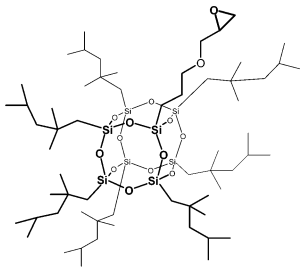

$POSS_{Oct}$E1

Networks with Monofunctional Pendant POSS. The networks with POSS dangling on the polymer backbones were prepared from the monoepoxide−POSS compounds with phenyl ($POSS_{Ph}$) or isooctyl ($POSS_{Oct}$) substituents. A fraction x of the epoxide groups from DGEBA of the reference network was replaced by epoxide groups from the monoepoxide−POSS, and the content of dangling POSS units in the network DGEBA(1−x)−POSS(x)−D2000 was controlled by the ratio of both epoxy monomers. The total amount of epoxy groups was kept constant and equal to the amount of NH hydrogen atoms in D2000.

Networks with Difunctional Pendant POSS. In the previous case, the incorporation of monofunctional monomers into the epoxy network leads to a decrease in cross-linking density compared to the reference DGEBA-D2000 network. To keep a constant cross-linking density, epoxy networks with pendant POSS were prepared by using diepoxide cyclopentane-substituted $POSS_{Cp-DGEBA}$ units (Hybrid Plastics). The amount of pendant POSSwas controlled by varying the ratio of the $POSS_{Cp-DGEBA}$ and DGEBA epoxy monomers (DGEBA(1−x)−$POSS_{Cp-DGEBA}$(x)−D2000). Besides the

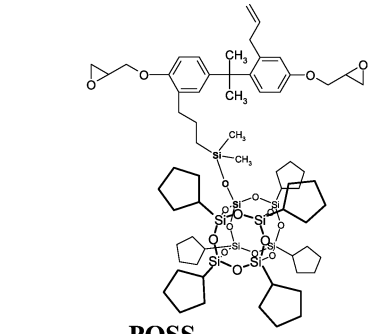

$POSS_{Cp\text{-}DGEBA,mono}$

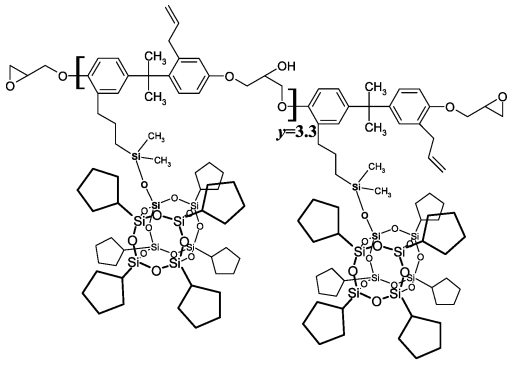

$POSS_{Cp\text{-}DGEBA,olig}$

$POSS_{Cp-DGEBA,mon}$ monomer containing on an average 1.6 POSS units per molecule we used also the oligomeric analog $POSS_{Cp-DGEBA,olig}$ that contains on an average 4.3 POSS units per molecule.

NMR Spectroscopy. Solid-state NMR spectra were measured using a Bruker Avance 500 WB/US NMR spectrometer (Karlsruhe, Germany, 2003) in 4 mm double-resonance probeheads at magic angle spinning (MAS) $\omega_r/2\pi = 12$ kHz with carrier frequencies 500.18, 125.78, and 99.37 MHz for ^{1}H, ^{13}C, and ^{29}Si nuclei, respectively. For the measurement of T_1 and $T_{1\rho}$ relaxation of ^{13}C magnetization in the rigid segments, standard relaxations experiments[30] with cross-polarizations (CP) were employed, while for the measurements of the relaxations of ^{13}C magnetization in mobile domains, the experiments with direct excitations were used (Scheme 1). The applied repetition delay between consecutive scans was 5 s. In the case of highly rigid systems the longer delay of 15 s was used. The intensity of excitation and spin-locking fields B_1(^{13}C, ^{29}Si) expressed in frequency units $\omega_1/2\pi = \gamma B_1$ was 64 kHz and the duration of cross-polarization contact time pulse was set to be 2 ms in all cases. The relaxation experiments were performed at two temperatures (297 and 315 K), and the temperature calibration correcting the frictional heating of samples was performed.[31] The site-specific measurements of one-bond ^{1}H−^{13}C dipolar couplings[32,33] under Lee−Goldburg conditions[34] were achieved by the "domain-selective"[20,21] amplitude-modulated (AM) PISEMA experiments[35,36] (Scheme 2). For the 2D ^{1}H−^{1}H correlation experiments, a MAS NOESY-type pulse sequence with a mixing period varied from 0.01 to 100 ms was applied, and the spinning frequency sufficient to remove dipolar broadening was 16−25 kHz (2.5 mm double-resonance probehead). The signals assignment in ^{13}C and ^{29}Si NMR spectra was performed on the basis of our previously published results.[29]

Results

The investigated epoxy−POSS nanocomposites were characterized by three sets of NMR experiments: First, the qualitative differences in mobility of molecular segments of the composites were studied by MAS and CP/MAS NMR measurements of ^{13}C and ^{29}Si nuclei, making possible to recognize "mobile" and "frozen" areas. Thereafter, the size of unbroken

Scheme 1. Schematic Representation of the Applied T_1 and $T_{1\rho}$ ^{13}C Relaxation Experiments

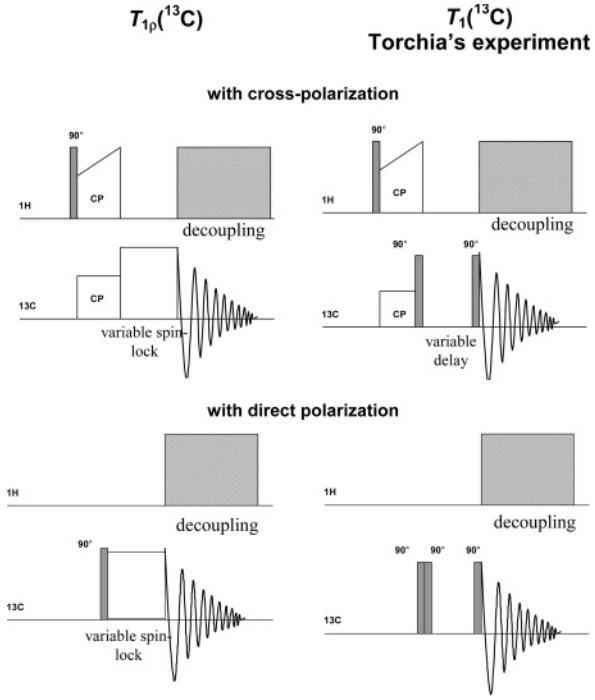

Scheme 2. Schematic Representation of the Applied "Domain-Selective" Recoupling Experiments: 2D T_1-Filtered AM−PISEMA Experiment, Selection of Rigid Domains (Upper Part); 2D Inverse T_1-Filtered Direct-Polarization AM−PISEMA Experiment, Selection of Mobile Domains (Lower Part)

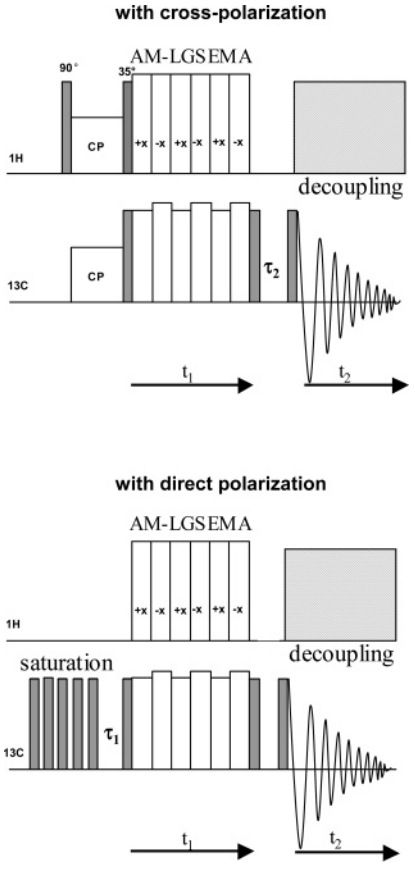

POSS domains was determined in 2D ^{1}H−^{1}H spin-diffusion experiments and the results were compared with the ones from previous works (SAXS, EM).[11] Finally, the molecular mobility was investigated in detail, by studying segmental motion

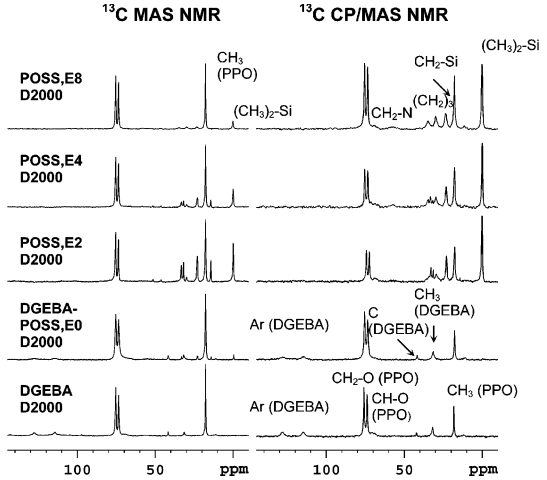

Figure 1. ^{13}C MAS and ^{13}C CP/MAS NMR spectra of the reference network DGEBA−D2000 and the epoxy networks modified by the POSS,E*n* units with variable functionality ($n = 0-8$).

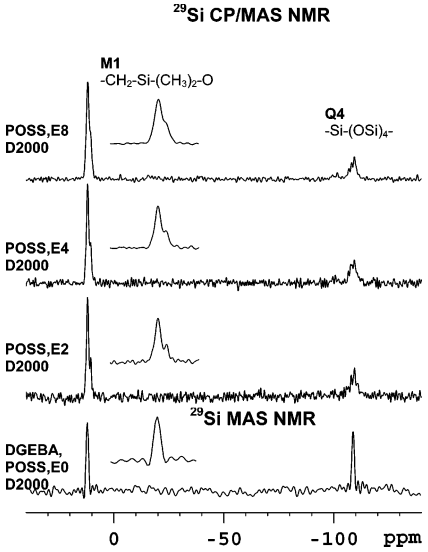

Figure 2. ^{29}Si MAS and ^{29}Si CP/MAS NMR spectra of the epoxy networks modified by POSS,E*n* units with variable functionality ($n = 0-8$).

frequencies and amplitudes in the high and low-frequency regions, thus giving a deeper insight into how the molecular dynamics of the various nanocomposites' components and of their segments influence the material properties (modulus, glass transition).

Qualitative Description of the Networks. ^{13}C and ^{29}Si NMR. At first, the qualitative differences in segmental mobility in the studied epoxy−POSS networks were determined: Polymer segments significantly differing in mobility can be simply distinguished by the comparison of solid-state NMR spectra carried out at two basic experimental regimes. A single-pulse MAS NMR experiment measured with a short repetition delay has the capability to acquire signals of rapidly relaxing flexible components, while the excitation of ^{13}C or ^{29}Si nuclei through the cross-polarization enhances signals of rigid segments.

This simple approach clearly revealed considerable motional heterogeneities (mostly) introduced by the incorporation of POSS units into the rubbery epoxy networks. The extent of the influence strongly depends on the functionality of POSS,E*n* building blocks. As indicated by the absence of the corresponding signals in ^{13}C CP/MAS NMR spectrum, the alkyl substituents of POSS,E0 units with zero functionality are isotropically moving and do not adopt the segmental dynamics of the PPO matrix (Figure 1). With increasing functionality, however, the intensity of these signals in ^{13}C CP/MAS NMR spectra increases indicating gradually restricted segmental mobility and formation of more rigid structures, while PPO segments still exhibit high dynamics. In the network modified by octafunctional POSS,E8 units, the POSS substituents' immobilization reaches such an extent that the T_1(^{13}C) relaxation is too slow for the ^{13}C spins fully relax during the repetition delay (4 s). Therefore, the corresponding signals in the single-pulse ^{13}C MAS NMR spectrum are suppressed (Figure 1, upper trace).

The isotropic tumbling of the whole POSS,E0 cages is definitely confirmed by the inefficiency of ^{1}H−^{29}Si cross-polarization and by the line-narrowing observed in the single-pulse ^{29}Si MAS NMR spectrum (Figure 2). On the other hand, the chemical bonding of the multifunctional POSS,E*n* units in the network causes splitting and asymmetric broadening of ^{29}Si NMR signals indicating magnetic nonequivalence of silicon atoms and symmetry distortion of POSS cages (details are discussed later).[37,38]

Regardless of the type of POSS substituents, the extensive formation of motional heterogeneities is observed for the systems modified by randomly incorporated monofunctional

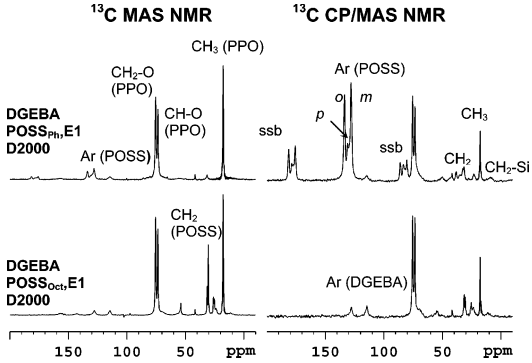

Figure 3. ^{13}C MAS and ^{13}C CP/MAS NMR spectra the epoxy networks modified by monofunctional POSS units (POSS$_{Oct}$, POSS$_{Ph}$) containing either isooctyl or phenyl inert substituents, respectively.

POSS$_{Oct}$ or POSS$_{Ph}$ compounds. As confirmed by ^{13}C NMR spectra (Figure 3), in both cases the siloxane cages do not adopt the motional state of the PPO matrix. In addition, PPO matrix itself exhibits motional heterogeneities. This is indicated by the differences in line width of PPO signals. In addition, the PPO matrix itself exhibits certain motional heterogeneities. This is indicated by the differences in line width of PPO signals. Owing to a high segmental dynamics and motional averaging of various conformations the mobile fraction of PPO matrix results in partially narrowed signals in ^{13}C MAS NMR spectrum while the same units exhibits slightly broader signals in ^{13}C CP/MAS NMR spectrum measured with cross-polarization. Although both the applied POSS$_{Ph}$ and POSS$_{Oct}$ units can be considered as freely dangling side groups, their behavior exhibits quite distinctive differences. While the POSS$_{Ph}$ units are substantially rigidified the PPO matrix remains elastic and mobile. This is indicated by the intensive signal enhancement of the signals of POSS$_{Ph}$ aromatic rings in ^{13}C CP/MAS NMR spectrum relatively to the signals of PPO blocks. On the other hand, due to the conformational variability of flexible alkyl groups the POSS$_{Oct}$ units exhibit higher internal dynamics in comparison with PPO matrix. Consequently the ^{1}H−^{29}Si cross-polarization is ineffective and only a small fraction of partially immobilized POSS$_{Oct}$ segments is indicated by low-intensive humps in a single-pulse ^{29}Si MAS NMR spectrum (Figure 4).

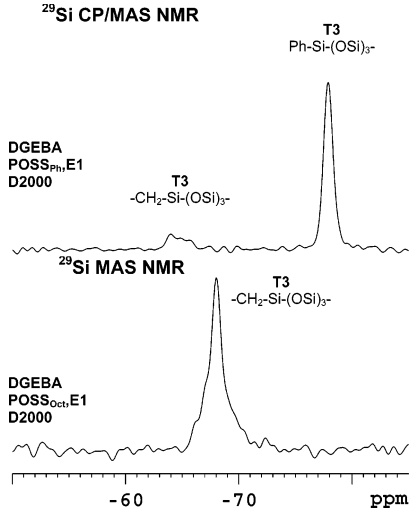

Figure 4. ^{29}Si MAS and ^{29}Si CP/MAS NMR spectra of the epoxy networks modified by monofunctional POSS units ($POSS_{Oct}$, $POSS_{Ph}$) containing either isooctyl or phenyl substituents, respectively.

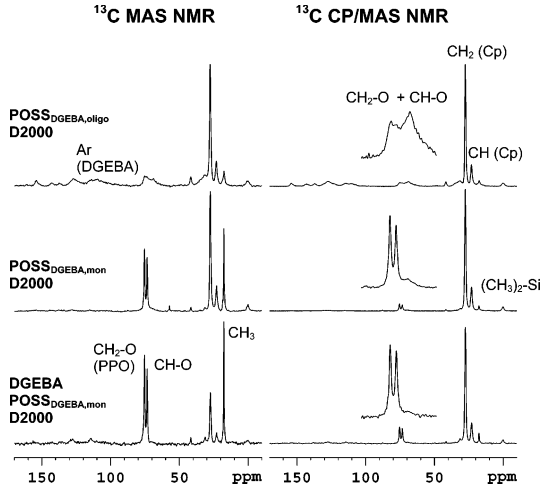

Figure 5. ^{13}C MAS and ^{13}C CP/MAS NMR spectra of the epoxy networks modified by diepoxide cyclopentane-substituted $POSS_{Cp-DGEBA,mon}$ and $POSS_{Cp-DGEBA,olig}$ units.

The increased probability that two dangling POSS units are located next to each other as regularly repeating substituents on a polymer backbone significantly supports immobilization of polymer segments. This is the very case of the epoxy networks modified by $POSS_{Cp-DGEBA,mon}$ and $POSS_{Cp-DGEBA,olig}$ compounds. The incorporation of "monomeric" $POSS_{Cp-DGEBA,mon}$ blocks leads to the formation of motionally heterogeneous networks, where the major fraction of PPO segments still remains in a highly mobile state while $POSS_{Cp-DGEBA,mon}$ units form rigid domains. This follows from the relative enhancement of the $POSS_{Cp}$ signals in ^{13}C CP/MAS NMR spectra. However, the modification of the epoxy network by oligomeric $POSS_{Cp-DGEBA,olig}$ diepoxide completely immobilizes the PPO matrix which adopts the motional behavior of $POSS_{Cp-DGEBA,olig}$ segments (Figure 5).

Similarly, as previously mentioned, the observed splitting of ^{29}Si NMR signals (Figure 6) reflects the magnetic nonequivalence of silicon atoms in $POSS_{DGEBA}$ building blocks. The signal analysis revealed the presence of three different types of Si atoms with the population ca. 3:3:1 which is in accord with the presence of two sets of three equivalent T3 silicon sites located around a C_3 symmetry axis[37,38] (Figure 6). The remaining T3 and Q4 silicon atoms then coincide with the symmetry axis.

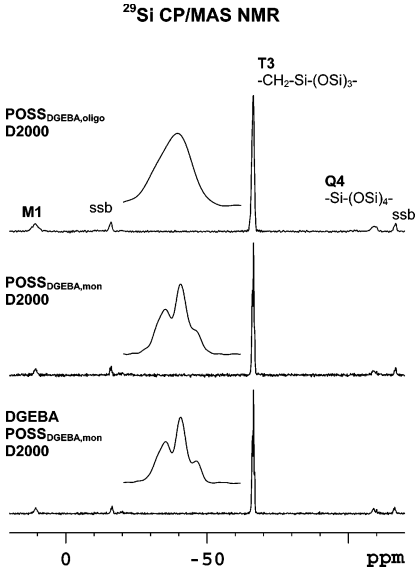

Figure 6. ^{29}Si CP/MAS NMR spectra of the epoxy networks modified by diepoxide cyclopentane-substituted $POSS_{Cp-DGEBA,mon}$ or $POSS_{Cp-DGEBA,olig}$ units.

The observed loss of the spectral resolution the system formed by oligomeric $POSS_{Cp-DGEBA,olig}$ segments probably indicates increased disorder of local arrangement of the $POSS_{DGEBA}$ units.

Local Order of Nanocomposite Networks via ^{1}H—^{1}H Correlation: Domain Size Determination. The successful development of polymer nanocomposites requires a deep analysis of self-assembling processes and the understanding of their impact on material properties. In order to assess the size of inorganic domains formed in the investigated nanocomposites, ^{1}H spin diffusion was probed and series of two-dimensional experiments correlating spatially close ^{1}H nuclei via through-space dipolar couplings were performed. In general, ^{1}H$-^1$H correlations allow tracing of interatomic contacts up to ca. 0.5 nm, and the analysis of ^{1}H spin diffusion makes it possible to probe the size of domains in heterogeneous systems up to a width of about 50 nm.[39] The success of such experiments is, however, preconditioned by a sufficient spectral resolution and requires the removal of the dipolar broadening. Besides various homodecoupling techniques,[40−42] a high-speed ^{1}H$-^1$H MAS NOESY-type experiment is an elegant way to access the required cross-peaks separation[43] (Figure 7).

Usually the spin diffusion between dipolarly coupled ^{1}H spins is traced through the dependence of correlation signal intensity on the mixing time. Applying the initial-rate approximation, this evolution is described by the second Fick's law, and assuming a simple two-component system, the size of the dispersed domains of the component *A* can be calculated according to the following equation:[39,44]

$$d_A = 2\frac{\epsilon}{f_B}\left(\frac{1}{\pi}Dt_{eq}\right)^{1/2} \quad (1)$$

Here f_B is the volume fraction of the continuous phase *B*, and t_{eq} is the time of magnetization equilibration, *D* is diffusivity, and ϵ reflects dimensionality of the process. The diffusivity, a parameter reflecting the average strength of dipolar couplings, was determined for every component in each polymer network. Using the previously described strategy,[45] knowing the effective size of an oxypropylene unit ($x = 0.35$ nm)[29] and assuming one-dimensional polarization transfer within the monomer unit ($\epsilon = 1$), the spin-diffusion coefficients attributed to PPO matrix

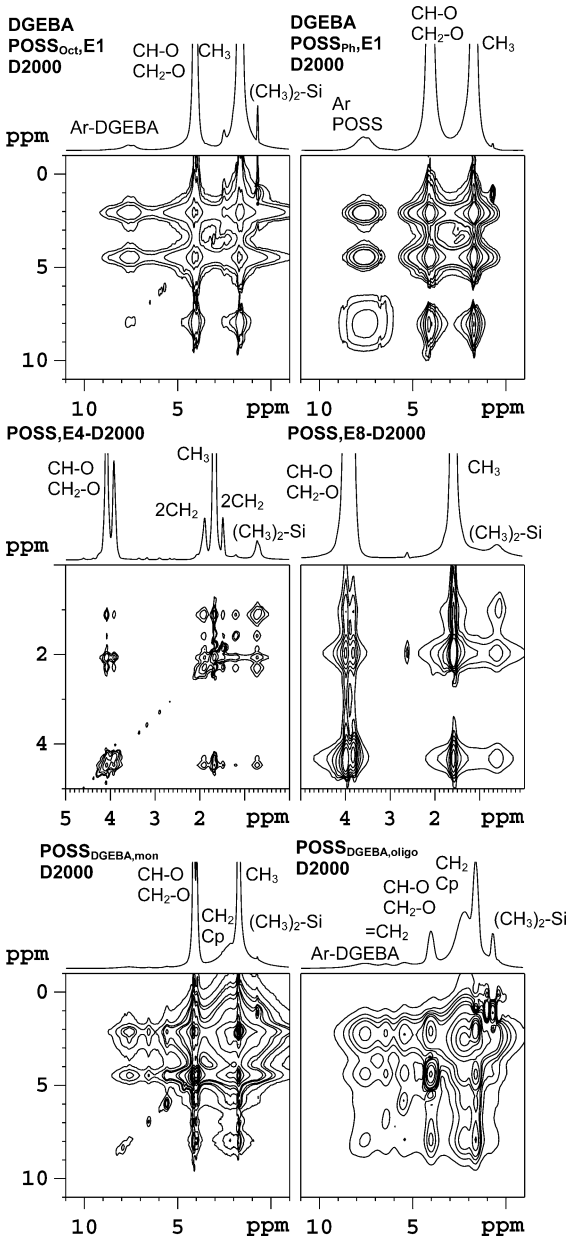

Figure 7. ^{1}H−^{1}H MAS correlation spectra of the selected POSS-reinforced networks recorded at 30 ms spin-diffusion mixing time.

were calculated from the equilibrium mixing times extracted from the buildup of the cross-peaks correlating CH_3 and CH_2−O protons[45,46] (Figures 7 and 8):

$$D = \frac{\pi x^2}{4\epsilon^2 t_{eq}} \tag{2}$$

Unfortunately, the absence of suitable correlation signals did not permit the measurement of diffusivity in POSS units. Owing to this fact, the coefficients for $POSS_{Ph}$, $POSS_{Cp}$, and POSS,E8 units were only estimated and assumed to be comparable with the diffusivity of the glassy PPO matrix in the $POSS_{Cp-DGEBA,olig}$−D2000 system ($D = 0.0962$ nm^2·ms^{-1}). The reliability of this assumption is supported by the fact that both PPO segments as well as POSS units in these systems are substantially rigidified. Finally, for the accurate analysis of spin diffusion in motionally heterogeneous systems, the effective diffusivity was calculated as an average value weighted by the volume fractions of individual components (Table 2).

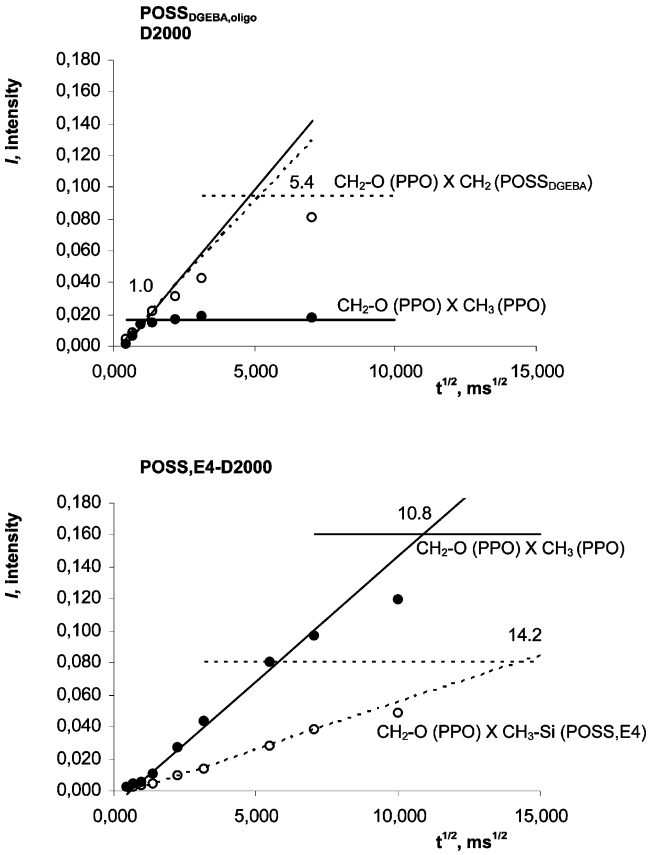

Figure 8. Spin-diffusion buildup curves obtained for $POSS_{DGEBA,oligo}$−D2000 and POSS,E4−D2000 networks demonstrating the evolution of cross-peaks correlating CH_2−O and CH_3 groups within PPO monomer units and for CH_2−O and CH_2 or CH_3−Si units between PPO and POSS building blocks.

Literature data[16,44,47] indicate that fast MAS averages out the dipolar interactions in such a way, that the effective diffusivities (D_{eff}) in these networks are comparable with the values determined for weakly ^{1}H−^{1}H-coupled mobile polyethylene oxide chains[47] or for sparse surface hydroxyls in siloxane networks.[16] However, the most demanding part of the domain size calculation is the estimate of the parameter of dimensionality (ϵ) reflecting shape of the dispersed particles. We assume rather imperfect assembling process of polymer blocks, which is why formation of deformed ellipsoidlike or rodlike aggregates characterized by the parameter $\epsilon = 2$ seems to be a compromise choice.

As demonstrated on the reference network the DGEBA segments are not significantly aggregated forming thus only very small domains with maximum diameter ca. 0.6−0.7 nm (this corresponds to ca. one or two DGEBA units). Somewhat larger chemically connected domains of tetrafunctional POSS,E4 blocks of the size about 1.5−2 nm (mainly single or double POSS,E4 units) can be expected in the POSS,E4−D2000 network. An additional increase in the size of domains is induced by the increase in POSS functionality, and octafunctional POSS,E8 blocks form domains which size is about 4−5 nm (corresponding to chemically connected clusters of several POSS units). Because of the high flexibility of alkyl chains in POSS,E0 and $POSS_{Oct}$ units the formation of a rigid phase is not allowed and rather liquidlike aggregates evolve. Consequently resulting ^{1}H−^{1}H dipolar couplings are motionaly averaged to zero, making impossible to measure the size of the arising domains. Roughly estimated from the observed nearly isotropic tumbling of the whole POSS cages in these systems,

Table 2. Times of Magnetization Equilibration between CH_3 and CH_2−O Protons within PPO Monomer Unit, t_{eq}(PPO), between CH_2−O Protons of PPO Units and POSS or DGEBA Blocks, t_{eq}, the Spin-Diffusion Coefficients of PPO Matrix, D_{PPO}, the Effective Spin-Diffusion Coefficients, D_{eff}, the Volume Fraction of PPO Matrix, f_{PPO}, and the Calculated Sizes of the Dispersed Domains, d

type of the network	t_{eq}(PPO) [ms]	D_{PPO} [nm^2·ms^{-1}]	f_{PPO}	t_{eq} [ms]	D_{eff} [nm^2·ms^{-1}]	d [nm]
DGEBA−D2000	5.9	0.0027	0.84	4.9	0.0027	0.6
POSS,E4−D2000	10.8	0.0008	0.54	14.2	0.0008	1.5
POSS,E8−D2000	12.7	0.0006	0.70	8.4	0.0293	4.7
DGEBA,$POSS_{Oct}$,E1−D2000	6.2	0.0024	0.84	6.4	0.0024	0.7
DGEBA,$POSS_{Ph}$,E1−D2000	6.5	0.0022	0.80	20.7	0.0215	8.5
$POSS_{DGEBA,mon}$−D2000	2.8	0.0118	0.59	21.2	0.0463	17.3
$POSS_{DGEBA,oligo}$−D2000	1.0	0.0962	0.25	5.4	0.0962	15.1

the intimate mixing of POSS,E0 or $POSS_{Oct}$ units with PPO matrix can be excluded. Instead, formation of large liquidlike droplets can be expected.

In contrast, due to the limited conformation variability and the ability of phenyl rings to participate in $\pi-\pi$ interactions, the $POSS_{Ph}$ units yield to a strong self-assembling process, leading to the formation of rigid relatively large domains (7−8 nm). Similarly, as a result of relatively strong hydrophobic interaction and favorable shape of cyclopentane substituents the largest domains reaching up to ca. 17−18 nm (Table 2) are created by $POSS_{Cp-DGEBA}$ segments.

Motional Frequencies of Polymer Segments. It has long been recognized that, besides the structure, also molecular dynamics covering a wide range of time scales, from picoseconds to seconds determine mechanical properties of polymers. The polymer chain dynamics exhibiting varying amplitudes and geometries, such as small-amplitude librations, aromatic ring flips or aliphatic side chains jumps can be characterized by an order parameter S (eqs 3−5) and a correlation time τ. In general, the order parameter S is a measure of the equilibrium distribution of orientations of the bond vector $\mu(t)$ in a molecular reference frame and ranges from 1 for fixed orientation to 0 for free motion.[48] In the simplest case, assuming a small-amplitude (θ) axially symmetric motion (so that $\langle \sin\theta \rangle \approx \langle\theta\rangle$), the order parameter can be converted[48,50,51] to the average fluctuation angle $\sqrt{\langle\theta^2\rangle}$:

$$S = 1 - \frac{3}{2}\langle\theta^2\rangle \tag{3}$$

For complicated motions other models providing more instructive pictures can be applied. For instance rapid jumps of the bond vector between N distinct orientations with populations p_i are analyzed according to the following relation:[48,51]

$$S = \sum_{i,j=1}^{N} p_i p_j P_2(\cos\theta_{ij}) \tag{4}$$

If the motion is modeled by the Gaussian axial fluctuation model,[52] the bond vector diffuses within a parabolic potential on the surface of a cone:

$$S = 1 - 3\sin^2\theta\{[\cos^2\theta(1 - \exp[-\sigma_f^2])] + 0.25\sin^2\theta(1 - \exp[-4\sigma_f^2])\} \tag{5}$$

where θ is the (fixed) angle between the bond vector $\mu(t)$ and the director axis for the motion and σ_f is the standard deviation of the fluctuation in the azimuthal angle.

That is why, after the qualitative characterization of molecular segment mobility, which revealed mobile and frozen areas in the PPO matrix, the motional dynamics of the investigated systems were studied in more detail. For this purpose, the frequencies of segmental motions were evaluated at first. Generally, two distinctive groups of segmental motions are easily recognized via spin relaxation mechanisms: High-frequency (ca. hundreds of MHz) motions (librations, rotations and jumps of small groups), and low-frequency motions (ca. tens of kHz) involving movements of larger parts of polymer chains. The high-frequency motions yield valuable "diagnostic" information about the situation of the corresponding groups in a material. They can support some slower motions, and they can influence intermolecular or intersegmental interactions. The low-frequency motions are known to correlate strongly with the thermomechanical material properties like modulus or glass transition and they can also absorb considerable amounts of mechanical energy.

An insight into the correlation times of both types of motions is provided by NMR relaxation measurements, which can examine segmental motions at two distinct time scales. The high-frequency motions are probed by the measurements of spin−lattice T_1 relaxation times at laboratory reference frame. Briefly speaking for the readers that are not familiar with NMR, T_1 relaxation is the process of recovery of a spin system into the thermodynamic equilibrium during which excitation energy ($\Delta E = h\gamma B_0/2\pi$) is dissipating into the lattice as heat, and a part of macroscopic magnetization (M_z) that is parallel with the direction of static magnetic field (B_0) exponentially decays. As the absorption of the excitation energy is not followed by spontaneous emission, the recovery must be forced by local segmental fluctuations which frequencies correspond with the absorbed energy: $\Delta E = h\omega_0/2\pi$ (ω_0 is the Larmor precession frequency, e.g., 125 MHz for ^{13}C spins at $B_0 = 11.7$ T). Consequently measurements of T_1 relaxation times of various nuclei starting from ^{1}H to ^{15}N cover a wide range of motional frequencies from ca. 500 to 50 MHz. Analysis of the low-frequency motions requires an application of significantly weaker magnetic fields. Experimentally, this is achieved by applying a rotating (spin-locking) B_1field which intensity expressed in frequency units is ranging from ca. 10 to 100 kHz (e.g., $\omega_1/2\pi = \gamma B_1 = 64$ kHz). If the measurement is performed in the coordinate system that is rotating with Larmor frequency ω_0, the static magnetic field apparently has not impact on the spin behavior. So the measurements of relaxation times at rotating frame ($T_{1\rho}$) open the window into the analysis of midkilohertz motions. The dependences between relaxation and correlation times are schematically depicted in Figure 9.

In order to probe the effect of POSS units on the behavior of polymer matrix, the T_1 and $T_{1\rho}$ relaxation times of −CH−O− groups of PPO segments were measured at various temperatures. Considering the existence of motional heterogeneities, two types of relaxation experiments were performed: the experiments with direct excitation of ^{13}C spins having capability to detect highly mobile segments, and the techniques based on the cross-polarization probing rigid polymer units. The justifiability of this approach is confirmed by the observed differences in $T_{1\rho}$ relaxation times (Table 3) that revealed remarkable differences

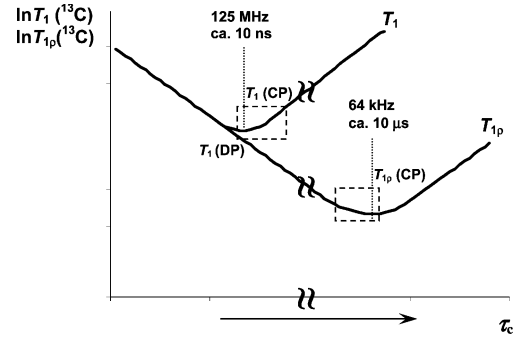

Figure 9. Schematic representation of the dependencies between relaxation times T_1 and correlation times τ_c (and/or inverse temperature $1/T$). The fastest relaxation is simply expected for segmental fluctuations with correlation frequencies close to resonant frequencies.

between mid-kilohertz frequency motions occurring in the "free" and in the "constrained" domains of the PPO matrix. Estimating correlation frequencies, the dependences of relaxation times on temperature prove, that nanosecond motions occur with correlation frequencies slightly below 125 MHz, while the correlation frequencies of microsecond motions are somewhat higher than 64 kHz (Figure 9, the probed regions are indicated by the dashed boxes).

The observed changes in relaxation times indicate that the modification of the reference network by multifunctional POSS,E*n* units causes a significant increase in correlation frequencies of segmental motions of PPO chins in both frequency regions. In the system containing bifunctional POSS,E2 units, the motional freedom reaches such a high extent, that the high-frequency motions exceed 125 MHz. With increasing functionality of POSS units the internal dynamics of the polymer matrix is gradually reduced to be nearing the reference network (DGEBA−D2000). However, not even the network modified by the octafunctional POSS,E8 blocks exhibits the same dynamics as the reference system.

The motional frequencies of the PPO matrix are nearly unaffected by the inert POSS,E0 blocks. The softening effect of liquidlike aggregates formed by these cages is very weak, leading only to a slight increase in motional frequencies. More pronounced softening of the network, is caused by the reduction of cross-linking density resulting from the incorporation of monofunctional $POSS_{Oct,}$E1 units. On the other hand, the presence of crystallites of phenyl-substituted $POSS_{Ph,}$E1 cages fully compensates for this effect.

Much more extensive changes in the relaxation behavior are observed in the systems modified by $POSS_{DGEBA}$ blocks, which maintain the same epoxide-functionality as DGEBA. Predominantly, the incorporation of $POSS_{DGEBA,mon}$ units is accompanied by the formation of a significant fraction of the "constrained" domains of PPO chains which exhibit significantly shorter $T_{1\rho}$ relaxation times. The observed enhancement in the relaxation efficiency indicates that motional frequencies of these segments are substantially reduced, approaching ca. 64 kHz. With increasing amounts of $POSS_{DGEBA}$ units, the fraction of the "constrained" domains increases. Finally the incorporation of oligomeric $POSS_{DGEBA,oligo}$ units leads to a complete immobilization of PPO chains in both frequency regimes.

Except the systems consisting with POSS,E2 and POSS,E4 blocks with nearly uniform motional behavior, the relaxation times listed in Table 4 indicate distinctive differences between the dynamics of PPO polymer matrix and POSS substituents. In contrast to soft droplike aggregates of POSS,E0 and $POSS_{Oct}$,E1, in solid aggregates the segmental motions are substantially hindered. However, the observed relaxation times are not extremely long indicating that certain flips and reorientations of POSS substituents in both main frequency regions outlive.

Motional Amplitudes. ^{1}H—^{13}C Dipolar Profiles. After characterizing the frequencies of segmental motions in the epoxy−POSS nanocomposites, it was of interest to determine the amplitudes of these motions. The recently developed ^{1}H−^{13}C separated-local-filed experiments (PILGRIM,[19] AM-PISEMA)[36] make straightforward the site-specific measurements of dipolar couplings, which contain information about the motional amplitudes of molecular segments. This is allowed by the fact, that any molecular motion with a correlation time shorter than ca. 40 μs causes averaging of one-bond ^{13}C−^{1}H dipolar interactions (ca. $\omega_D/2\pi = 25$ kHz). Then the ratio of a motionally averaged dipolar coupling constant (D_{CH}) and the rigid-limit value ($D_{CH,rig}$) defines an order parameter (S) that can be converted to the amplitude of segmental motion[48] (eqs 3−5). Following from the experimental Lee-Goldburg condition,[34] the scaling factor cos(54.7°) reduces the rigid-limit value of a typical one-bond C−H pair to be ca. 13.2 kHz, however, owing to the experimental imperfections, the rigid-limit value is a bit smaller: ca. 12.0−12.5 kHz. That is why before every experiment, a model compound measurement (L-Ala) was performed. The order parameters were estimated from the dipolar profiles of CH and CH_2 groups since the dominant splittings observed in the dipolar spectra reflect spin-pair one-bond ^{13}C−^{1}H dipolar couplings as confirmed by the previous spectral simulations.[49] The influence of additional remote spin was also tested and it has been found out that the dipolar profiles of CH and CH_2 groups are still dominated by one-bond dipolar couplings and multispin behavior can be neglected. This confirms that spin-pair analysis is suitable approach also for the typical organic polymers with a dense proton network (for the details and simulated dipolar profiles, see Supporting Information).

To probe motional amplitudes in the "free" and "constrained" domains separately, we applied the recently developed "domain-selective" AM-PISEMA experiments[20,21] (Scheme 2) that select ^{13}C magnetization of either rapidly or slowly relaxing components. As the differences in T_1 relaxation times in various PPO domains are not extremely large, the applied relaxation filters only partially suppress the unwanted ^{13}C magnetization. Despite this fact, the dominant narrow signals reflecting mobile PPO chains in the "free" domains (Figure 10) are removed, allowing the emergence of the broad doublets of rigid units in the "constrained" PPO domains (Figure 11). However, the zero-frequency signals must be interpreted very cautiously because they originate from a mixture of many contributions like long-range ^{1}H−^{13}C dipolar interactions or incompletely refocused homonuclear ^{1}H−^{1}H dipolar couplings.[32,33] In addition, above T_g, the transitions between all the conformations take place on the same time scale as rotational motions involving small-step diffusion and jumps by arbitrary angles.[53] Consequently, geometry of the motion in the "free" domains cannot be described by employing a fixed diamond lattice,[53] and the application of the above-mentioned models is speculative.

Nevertheless, for a comparative study of related systems, the discrete transitions *gauche*$^+$−*trans*−*gauche*$^-$ (g^+-t-g^-) can be considered as a fundamental motional mode, on which other motions are superimposed. Theoretically, the three-site jumps between g^+-t-g^- conformations with equal populations reduces the order parameter to the value $S = 0.11$ ($\theta_{ij} = 109°$, $p_i = p_j = p_k = 0.333$, eq 4). That is why the narrowing of the central signals (Figure 10) below this value can be interpreted as an increase in the freedom of large amplitude rotational-

Table 3. $T_1(^{13}C)$, $T_{1\rho}(^{13}C)$ Relaxation Times of −CH−O Groups of PPO Units Measured at 297 and 315 K by the Experiments with Cross-Polarization (CP) and Direct Polarization (DP) of ^{13}C Spins (Scheme 1)

	297 K				315K			
	T_1		$T_{1\rho}$		T_1		$T_{1\rho}$	
type of the network	CP [s]	DP [s]	CP [ms]	DP [ms]	CP [s]	DP [s]	CP [ms]	DP [ms]
reference network								
DGEBA−D2000	0.61	0.56	6	7	0.47	0.39	10	22
networks with POSS in junctions								
POSS,E8−D2000	0.47	0.41	8	24	0.41	0.38	24	44
POSS,E4−D2000	0.42	0.40	13	25	0.40	0.38	25	49
network with POSS in chain backbone								
POSS,E2−D2000	0.34	0.39	15	32	0.35	0.43	30	57
network with nonbonded POSS nanofiller								
DGEBA,POSS,E0−D2000	0.57	0.52	7	10	0.40	0.41	13	25
networks with monofunctional pendent POSS								
DGEBA,$POSS_{Ph,}$E1−D2000	0.63	0.57	5	6	0.47	0.43	12	23
DGEBA,$POSS_{Oct,}$E1−D2000	0.52	0.46	7	11	0.40	0.35	19	35
networks with difunctional pendent POSS								
DGEBA,$POSS_{DGEBA,m}$−D2000	0.63	0.59	6/0.8[a] 1/0.2[a]	8/0.8[a] 2/0.2[a]	0.51	0.44	13/0.9[a] 1/0.1[a]	20/0.9[a] 2/0.1[a]
$POSS_{DGEBA,mon}$−D2000	0.62	0.61	7/0.5[a] 2/0.5[a]	7/0.6[a] 2/0.4[a]	0.50	0.46	13/0.8[a] 1/0.2[a]	15/0.8[a] 2/0.2[a]
$POSS_{DGEBA,oligo}$−D2000	3.12	3.15	8	8	1.25	1.22	4	4

[a] The double-component $T_{1\rho}(^{13}C)$ relaxation: the first figure represents the relaxation time in ms, while the relative amplitude of the corresponding component is indicated by the second figure.

Table 4. $T_1(^{13}C)$, $T_{1\rho}(^{13}C)$ Relaxation Times of POSS Substituents in Aggregates Measured by Standard Relaxation Experiments with Cross-Polarization (CP) at 297 and 315 K

			297 K		315 K	
type of the network	group	$\delta(^{13}C)$ [ppm]	T_1 [s]	$T_{1\rho}$ [ms]	T_1 [s]	$T_{1\rho}$ [ms]
POSS,E8−D2000	CH_2	23	1.29	4	1.05	8
	CH_2	32	1.27	4	1.09	9
POSS,E4−D2000	CH_2	23	0.55	6	0.52	10
	CH_2	32	0.52	5	0.45	11
POSS,E2−D2000	CH_2	23	0.41	8	0.44	12
	CH_2	32	0.39	10	0.43	13
DGEBA,$POSS_{Ph,}$E1−D2000	CH═	134	3.7	21	3.7	29
	CH═	130	4.0	37	4.1	41
$POSS_{DGEBA,mon}$−D2000	CH	23	1.2	20	1.1	22
	CH_2	28	1.4	17	1.5	20
$POSS_{DGEBA,oligo}$−D2000	CH	23	1.1	29	1.2	32
	CH_2	28	1.6	24	1.8	28

diffusion motions involving higher number of polymer segments (systems modified by noncrystallizable POSS units). Oppositely, in the networks where POSS blocks form rigid chemical or physical aggregates, these motions are hindered and the overall amount of the "free" domains decreases (e.g., $POSS_{DGEBA,oligo}$−D2000 system).

In the "constrained" domains, the motional amplitudes of PPO chains are remarkably restricted (Figure 11). For instance the increased order parameter can be explained by unequal populations of various conformations g^+, t, and g^- (e.g., DGEBA−D2000, $S = 0.25$). The sterical shielding in these domains can reach the limit when two-site jump motions ($g \leftrightarrow t$) start to dominate (e.g., POSS,E8−D2000, $S = 0.33$, $\theta_{ij} = 109°$, $p_i = p_j = 0.5$, eq 4). As reflected by broadened dipolar profiles, a relatively wide range of motional amplitudes can be expected. In particular, in the system modified by octafunctional POSS,E8 cross-links, the additional "extra-constrained" domains reflected by the outer dipolar doublet were found. In this case, assuming axially symmetric rotational-diffusion motion, the order parameter $S = 0.92$ indicates small-amplitude wobbling with the average fluctuation angle of CH vectors about $\theta = 13°$ (eq 3). Similar but less apparent features are observed also for the system DGEBA,$POSS_{Ph,}$E1−D2000. The influence of the number of potentially crystallizable POSS units on the motional amplitudes of the confined PPO chains is demonstrated

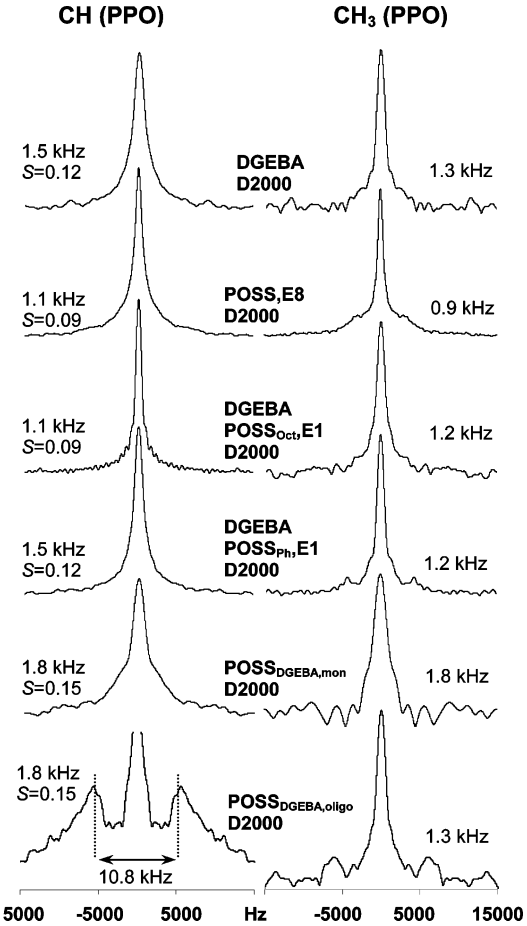

Figure 10. Inverse-T_1-filtered dipolar spectra recorded for CH and CH_3 units of PPO chains in the "free" domains. The full-widths at half-height of the signals are shown at the left or right side of each spectrum while the corresponding order parameters S are listed left.

on the systems modified by $POSS_{DGEBA}$ units. While in the "constrained" domains of $POSS_{DGEBA,mon}$−D2000 network (68 wt % of POSS epoxide) still high-amplitude two-site $g \leftrightarrow t$ jumps prevail ($S = 0.35$, $\theta_{ij} = 109°$, $p_i = p_j = 0.5$, eq 4), modification of the network by $POSS_{DGEBA,oligo}$ units (88 wt %

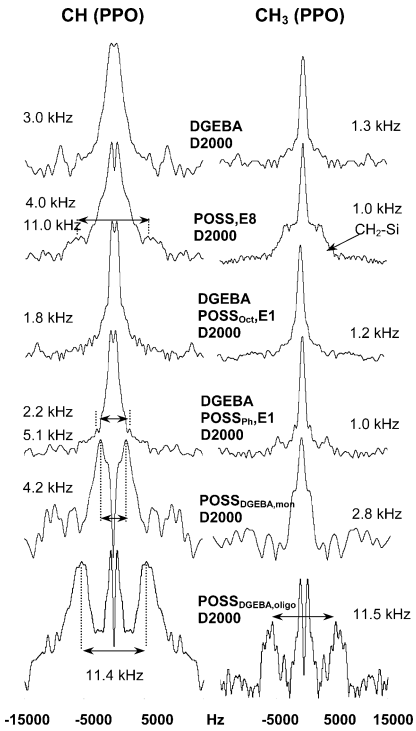

Figure 11. T_1-filtered dipolar spectra of CH and CH_3 units recorded for the confined PPO chains. The motionally averaged splittings in kHz ($\Delta\nu$) reflecting dipolar couplings (D_{CH}) are shown at the left/right side of each spectrum.

of POSS epoxide) leads to a complete immobilization of PPO segments ($S = 0.95$, $\theta = 10°$, eq 3). The sterical restriction in the later system is so extensive that also methyl rotation in the confined PPO chains is reduced (Figure 11, right column).

In the same way, the dipolar profiles of rigid segments in the POSS aggregates were recorded (Figure 12). Although the global dynamics of $POSS_{Ph}$ and $POSS_{Cp-DGEBA}$ cages must be reduced to form crystallites,[11] the motional amplitudes of the organic substituents are surprisingly high. To explain very small order parameter ($S = 0.35$) of ortho/meta CH═ groups in phenyl rings a simultaneous action of several motion modes must be supposed. The two-site 180° flip reduces the order parameter to only $S = 0.5$ ($\theta_{ij} = 120°$, $p_i = p_j = 0.5$, eq 4). That is why additional contributions must be taken into account. At first the spin-pair dipolar interactions under the large-amplitude motion can no longer be considered as axially symmetric ($\eta = 1.0$). For the two-site 180° phenylene ring flip the asymmetry parameter ($\eta = 0.6$) scales down the theoretical order parameter to ca. $S = 0.44$.[19] As this scaling still cannot fully explain the observed behavior, the second motional mode of phenylene rings was considered. With a high probability, the flip axis is not stable but undergo a certain libration which is evidenced by the order parameter of the CH═ unit in the para position ($S = 0.72$). Theoretically, in the case of a fixed axis, the order parameter should be unreduced ($S = 1$). That is why the wobbling of the whole phenylene group in the direction up and down the plain of aromatic ring with an average fluctuation angle ca. $\theta = 25°$ can be supposed as one of the possible additional motional modes (eq 3, Scheme 3a).

A bit more restrained motions were found in $POSS_{DGEBA}$ crystallites. Taking into account the rigid lattice of Si and O atoms and the geometry of cyclopentyl substituents, the Gaussian axial fluctuation model (eq 5) is a suitable choice for the analysis of the order parameter of CH groups ($S = 0.45$). With the cone semi-angle ($\theta = 109°$) defined by −Si−C−H bond angle, the

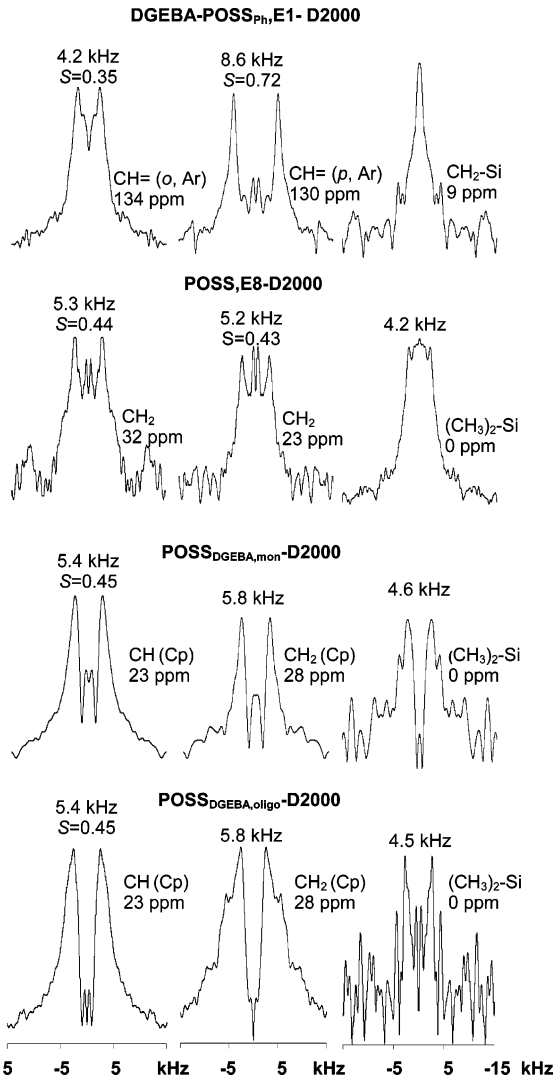

Figure 12. T_1-filtered dipolar spectra of substituents of POSS cages. For better identification, every structure unit is assigned to ^{13}C NMR chemical shift.

applied model predicts diffusion of the C−H vector within a parabolic potential on the cone surface with the average fluctuation angle ca. $\sigma_f = 35°$ (Scheme 3b). As indicated by the order parameters of CH_2 groups ($S = 0.43-0.45$, Figure 12), restrained motions with similar amplitudes can be expected also for the hexyl spacers linking POSS,E8 or POSS,E4 cages with the PPO matrix. Although these POSS,E8(E4) cages do not form crystalline domains, a tight packing is evidenced by the reduced rotation of $Si-(CH_3)_2$ methyl groups (Figure 12).

Discussion

This work complements the recent studies[11,12] of morphology and mechanical properties of epoxy networks based on DGEBA cross-linked PPO chains reinforced by POSS cages−polymer nanocomposites exhibiting complicated architecture. The current analysis highlights motional heterogeneities and differences in segmental mobility in various polymer domains in order to correlate molecular properties with macroscopic and thermo-mechanical behavior of these nanocomposites.

The understanding of basic structural motifs in the reference DGEBA−D2000 system is the starting point for the elucidation of POSS effects. The high rate of polyaddition reactions of the DGEBA oxirane rings with primary amines supports the formation of the infinite "poly(aminoDGEBA)" chains that are

Scheme 3. Schematic Representation of Segmental Motions in the Crystallites of $POSS_{Ph}$ (a) and $POSS_{Cp}$ Units (b)

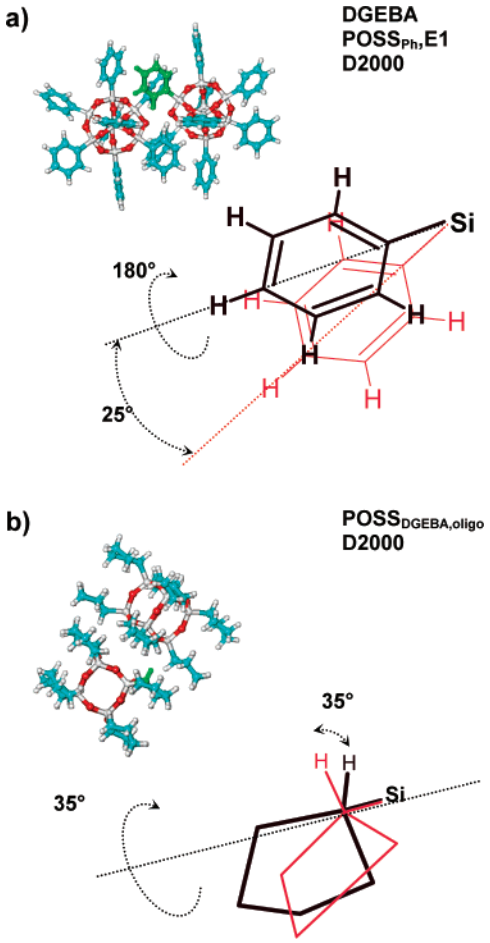

Scheme 4. Schematic Representation of the Reference Network DGEBA−D2000 (a) and the DGEBA−$POSS_{Ph}$,E1−D2000 Network with Randomly Incorporated $POSS_{Ph}$ Units (b) and with Aggregated $POSS_{Ph}$ Units (c)

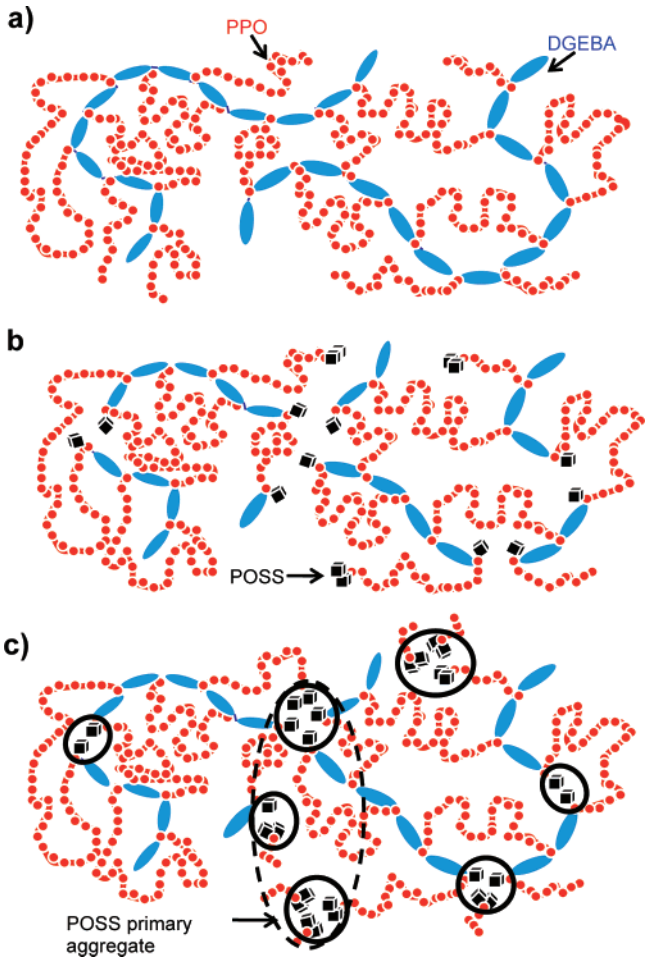

interconnected by flexible PPO blocks (Scheme 4a). Already this arrangement induces motional heterogeneities because the conformational flexibility of poly(aminoDBEGA) chains and of closely neighboring PPO segments is reduced. Additional sources of motional defect are introduced by randomly incorporated monofunctional $POSS_{Ph}$ or $POSS_{Oct}$ units that terminate poly(aminoDGEBA) chains (Scheme 4b). Consequently, the cross-linking density is reduced and the shorter poly(aminoDGEBA) segments exhibit increased mobility. On the other hand, due to the recently described polymerization-induced phase separation[54] and due to the preferential interaction of POSS substituents (e.g., $\pi-\pi$ stacking), POSS units aggregate to form bulky and structurally complicated physical junctions (Scheme 4c), which, in the case that they are crystalline, substantially reduce the mobility.

Previous SAXS and TEM measurements[11] revealed the size of crystallites of $POSS_{Ph}$ units to be ca. 30 nm, while our spin-diffusion experiments found the domains to be significantly smaller (ca. 8 nm). This difference partly results from the fact that the spin-diffusion experiments generally underestimate the size of the dispersed particles.[44] However, at the same time, we can assume the fine internal structuring of the $POSS_{Ph}$ aggregates. In fact it is hard to imagine formation of the 30 nm size domains of $POSS_{Ph}$ cages that do not contain directly incorporated chemically bonded PPO fragments. Instead, the large $POSS_{Ph}$ aggregates detected by SAXS consist with smaller crystallites that are separated by PPO segments.

From the macroscopic point of view, due to the crystalline state of the $POSS_{Ph}$ aggregates the formed physical cross-links easily compensate the lower cross-linking density and substantially enhance the storage modulus (12 MPa) in the rubber region. This phenomenon, however, is not accompanied by the decrease in segmental dynamics of the PPO matrix (T_g is unaffected). The absence of confined chains is somewhat surprising, because the interfacial area between nanometer-sized $POSS_{Ph}$ crystallites and PPO matrix must be relatively large. This behavior can be explained by the high-amplitude flips of phenyl rings that make interfacial interactions with PPO chains ineffective. Considering the phenyl flips, the $POSS_{Ph}$ crystallites play not only the role as physical cross-links but they also can absorb large amounts of mechanical energy. In general, the high-amplitude phenyl flips are considered to be mechanically active, providing thus the molecular source of high ductility of many polymers. That is why the balance between $\pi-\pi$ interactions and phenyl flips can be considered as a potential factor supporting improvement in mechanical properties.

On the other hand, the reduced cross-linking density itself causes a decrease in dynamic shear storage modulus (from 3 to 0.9 MPa) and glass transition temperature (from −29 to −31 °C; DGEBA−$POSS_{Oct}$,E1−D2000). Probing motional frequencies of PPO chains, we observe only a small increase in midkilohertz and megahertz regions, while motional amplitudes are released, tending to reach an isotropic state. This results from the absence of the constrained domains of PPO chains due to the fragmentation of poly(aminoDGEBA) chains. In addition, due to the weak cohesion forces, the physical junctions formed by soft $POSS_{Oct}$ aggregates are not able to compensate

Scheme 5. Schematic Representation of the $POSS_{Cp-DGEBA,olig}$−D2000 Network

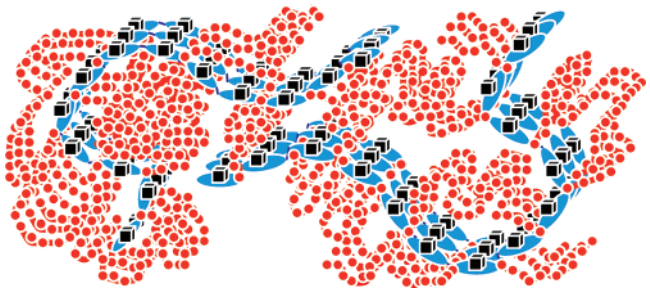

the missing chemical cross-links. This indicates that the presence of even relatively large amount (30 wt %) of bulky POSS units may not always affect the dynamics of flexible polymer chains, and the role of POSS unit as an anchor is not general.

The situation is quite different in $POSS_{Cp-DGEBA}$−D2000 systems, where the POSS cages do not reduce cross-linking density but form regular substitutents of polymer backbone. This arrangement offers preferential aggregation of parallel chains into the POSS-rich crystallites separated by PPO segments (Scheme 5). As the sizes of these crystallites determined by spin-diffusion measurements (15−17 nm) and X-ray diffraction scattering (ca. 19 nm) are in accord, the PPO chains are not involved in the crystallites but rather form their surroundings. At room temperature, the network $POSS_{Cp-DGEBA,mon}$−D2000 shows an increase in modulus by 1.5 order of magnitude while the incorporation of longer sequences of $POSS_{Cp-DGEBA,olig}$ causes an increase in modulus by ca. 2 orders with respect to the reference network. This enhancement can be attributed not only to the formation of physical junctions but also to the presence of the "constrained" domains of PPO chains in which high-amplitude motions are reduced. This immobilization can reach such an extent that PPO segments undergo only small amplitude wobbling, with an average fluctuation angle that is comparable with the motional amplitudes of polyamide-6 chains in crystallites.[21] This indicates tight and perhaps regular arrangement of PPO chains, which additionally contributes to the enhancement of the storage shear modulus.

In contrast to the simple reference system DGEBA−D2000, for which a slight temperature-induced increase in modulus—resulting from the entropic elasticity of PPO chains—is observed in the rubber region, the $POSS_{Cp-DGEBA}$−D2000 networks exhibit a steep modulus decrease in that region. This mainly results form the disordering of polymer segments, that predominantly occurs in the "constrained" domains of PPO chains, while $POSS_{Cp-DGEBA}$ crystallites seem to be less affected by the heating. This statement follows from the variable-temperature relaxation experiments revealing significant changes in $T_{1\rho}$ relaxation times of PPO segments only. The stability of $POSS_{Cp-DGEBA}$ crystallites may result from the ability of cyclopentyl substituents to convert thermal energy into segmental motion.

In most of the samples investigated, the presence of POSS aggregates has only little effect on T_g. This is probably given by the weak interactions between POSS domains and PPO matrix. The glass transition temperature is rather determined by the stiff poly(aminoDGEBA) chains, ideally interpenetrating through the whole systems, because the cleavage of these chains causes a dramatic decrease in T_g. A mild but significant increase in glass transition temperature is observed only if POSS units are regularly attached on poly(aminoDGEBA) chains, the flexibility of which is thus reduced. In the case of the extremely stiff $POSS_{Cp-DGEBA,olig}$, the effect on T_g of replacing DGEBA

Scheme 6. Schematic Representation of POSS,E2−D2000 System (a) and the More Realistic Picture Where POSS,E4 Units Form Chemically Bonded Clusters (Fragments of the Theoretical 3D Poly(POSS) Network) as Well as Linear Units (b)

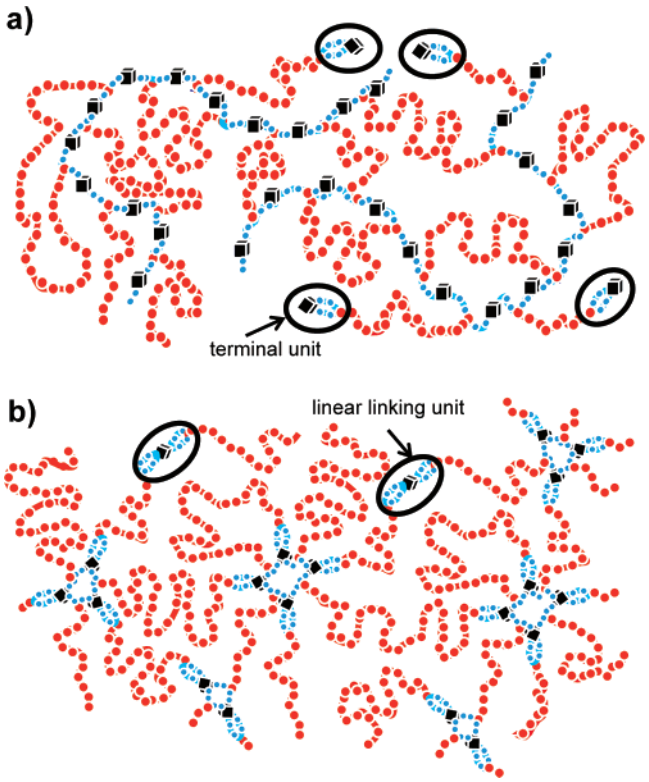

by these units is very strong, and a marked immobilization of PPO chains is also observed (Figure 11).

The dominant role of poly(aminoDGEBA) chains on the thermomechanical behavior of PPO matrix is demonstrated on the networks containing multifunctional $POSS,E_n$ building blocks and Jefamine D2000. The simplest POSS,E2−D2000 network, in which difunctional POSS cages form infinite "poly(POSS)" chains (Scheme 6a), is an analogue of the DGEBA−D2000 reference system. Although the cross-linking functionalities of the POSS,E2−D2000 network and of the reference system are identical, the significantly higher flexibility of "poly(POSS)" chains dramatically reduces not only the storage modulus to 0.2 MPa but also T_g to −75 °C. The conformational freedom of these chains is so high, that the PPO segments exhibit nearly isotropic tumbling with correlation frequencies exceeding the limit of 125 MHz.

An increased functionality of POSS,E*n* segments makes the arising structures much more complex and one can imagine several structural motifs. For instance, the reaction of two oxirane rings stemming from the same POSS,E2 unit with a $-NH_2$ group lead to the termination of PPO chains (Scheme 6a). Generally, such a "cyclic bonding" of NH_2 groups to multifunctional POSS epoxides is sterically more favorable (Scheme 7) than the "ideal", "network-constructing" reaction, in which two epoxy groups from different POSS units react with one NH_2 group. Analogous reactions of POSS,E4 cages lead to trifunctional or even to linear linking POSS units (Scheme 6b). In the E8−D2000 system, the "cyclic bonding" of epoxy substituents of E8 to NH_2 groups of D2000 can reduce the effective functionality to 4 (from the original 8). The probability of the described "cyclic bonding" increases with increasing POSS functionality. Hence, the multiple-functionality of POSS,E*n* cages typically is not fully utilized and the

Scheme 7. Reactions of Multifunctional POSS,E*n* Epoxide with a Primary Amine: (1) "Ideal Reaction" Connecting Two POSS Units (top) and (2) "Cyclic Bonding" of One POSS Unit to the Amino Group

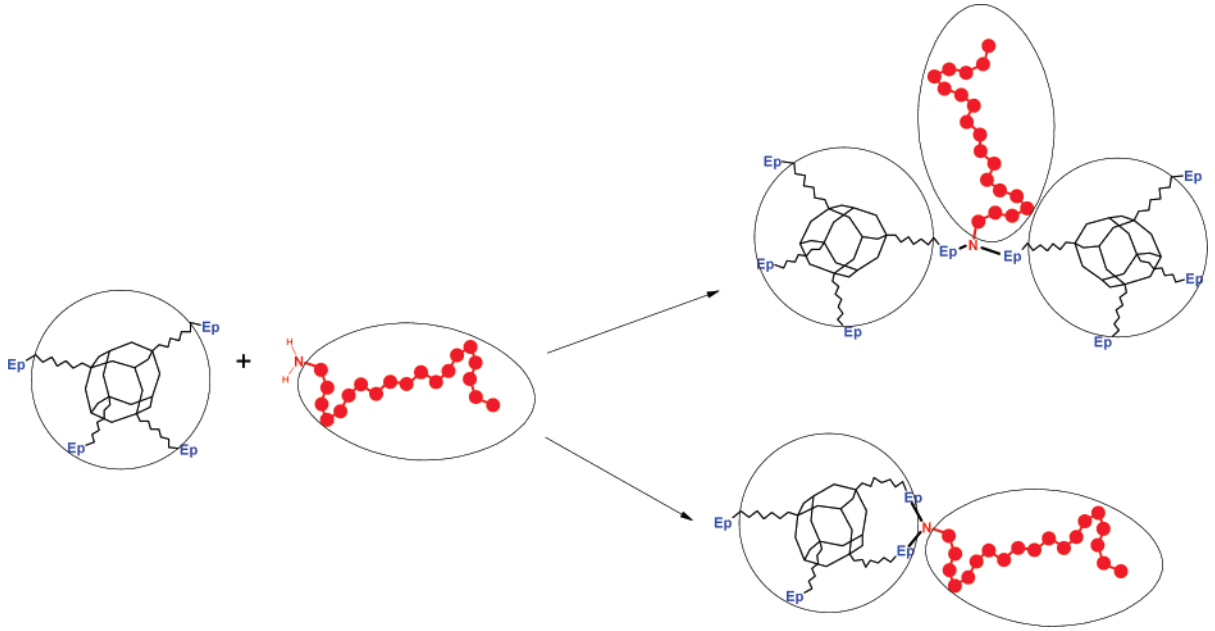

reinforcing of the network cannot reach the theoretic maximum values.

An "ideal cross-linking" of the POSS,E*n* cages would lead to the formation of an infinite 3D network (as shown in Scheme 8 for POSS,E4) which would contain an infinite 3D structure made from POSS units connected by N atoms from the PPO's NH_2 groups. The rigid poly(amino−POSS) network would be further interpenetrated by PPO chains connecting N atoms of the network. Because of the described arrangement, the PPO chains would possess no elastic activity any more and the whole "ideal network" would be hard and glassy. The formation of the ideal network, however, is prevented not only by the above-discussed nonideal cyclic bonding, but is even impossible due to sterical reasons (see Scheme 8). The poly(amino−POSS) structure would already fill most of the space available, leaving practically no place for the PPO chains, which in the systems investigated need more space than the POSS units, as D2000 has a similar MW but a lower density. The above-discussed effects lead to a clustered, nanoheterogeneous structure of the E4−D2000 and E8−D2000 networks[55] in which the chemical clusters of POSS units can be considered as small fragments of the "ideal network" with entrapped and rigidified PPO chains ("extra-constrained" domains, Figure 11).

The enhancement in mechanical properties induced by the increase in functionality of POSS,E*n* units is not dramatic. Even utilizing octa-functional POSS,E8 segments, the glass transition temperature still remains 16 °C below the T_g of the reference network, and the storage shear modulus (3.8 MPa) only two times exceeds the original value (2.0 MPa), in spite of much higher network functionality. This relatively weak modulus enhancement results from the network structure depicted in Scheme 6b, in which the somewhat rigid poly(amino−DGEBA) chains of the reference network are missing. In addition the size of the hard 3D poly(amino−POSS) fragments of the "ideal network" was found to be smaller than 5 nm (corresponding to several POSS units per aggregate). In these fragments only a small fraction of strongly immobilized PPO chains undergoing to only small-amplitude librations of about 10° is entrapped. In general such clusters have potential to enhance mechanical strength. However, these "extra-constrained" domains are completely separated by a continuous phase of PPO matrix exhibiting almost unrestricted high-amplitude dynamics. Consequently

Scheme 8. Simplified (Highly Regular for Simplicity) Structure of an Ideal POSS,E4-D2000 Network with a Maximum Use of Functionality of the Components: Connectivity in Detail (Top) and a Larger Structure (Stretched in Height) Fragment, on Which the Sterical Problems Are Highlighted (Bottom)

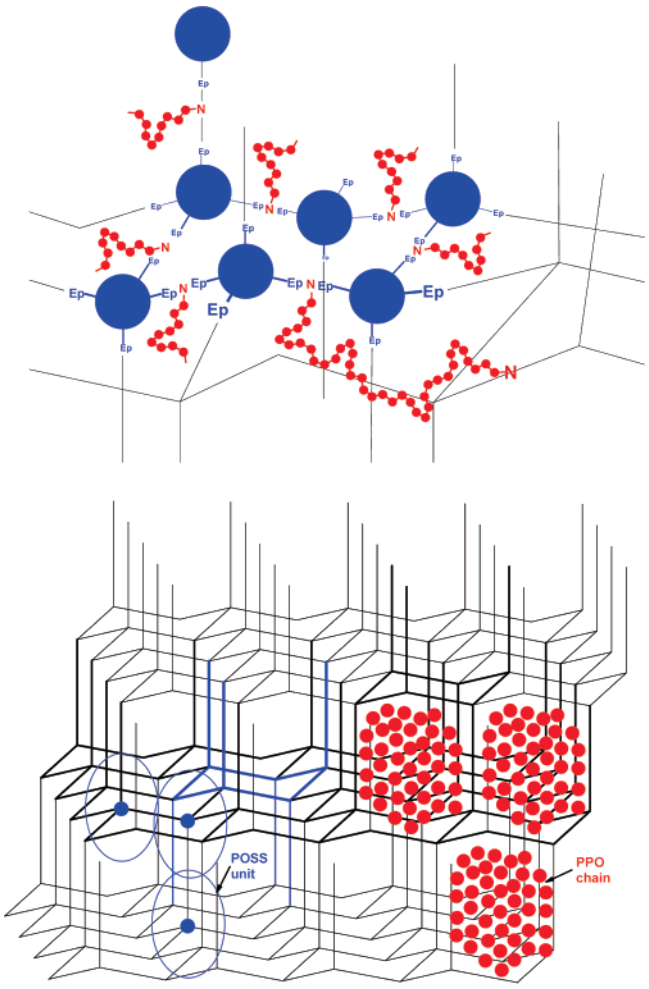

the effect of restricted mobility is not propagated into the more distant polymer chains and that is why the shear storage modulus, as well as the glass transition temperature are only slightly affected, and the whole system exhibits entropic elasticity.[11,12]

Conclusions

In this contribution, it is demonstrated that a combination of traditional tools of solid-state NMR spectroscopy with recently developed recoupling techniques opens new ways to describe and understand relations between structure, segmental dynamics, and macroscopic properties in complicated polymer systems like nanocomposites. A typical example of these systems with hierarchical architecture was provided by polymer networks based on poly(propylene oxide) chains (PPO) cross-linked by diglycidyl ether of Bisphenol A (DGEBA) reinforced by polycyclic oligomeric silsesquioxanes (POSS). The tendency to aggregation and self-organization of individual building blocks was qualitatively and quantitatively described, and multilevel ordering was revealed by $^1H-^1H$ spin-diffusion experiments. The spin-diffusion experiments yielded the size of unbroken domains in the nanocomposites, offering an alternative to the established methods like electron microscopy (EM), SAXS, or AFM. This approach made possible distinction of the primary domains from "aggregates of primary domains", the size of the latter being measured by EM or SAXS. Generally, a good agreement was found between the presented results and domain size measured on the investigated nanocomposites previously by SAXS and EM. In one case the domain size determined by NMR was several times smaller than that by SAXS or EM, implying the presence of "broken domains" ("aggregates of aggregates", with the chains of the polymer matrix separating the small primary domains).

Mobility investigations via NMR were shown to yield valuable information about molecular dynamics, making possible the assignment of the contribution of individual molecular segments to thermomechanical properties or predicting the materials' ability of absorbing mechanical energy. It was clearly confirmed that the resulting networks structure and morphology, containing either chemical or physical POSS aggregates, leads to remarkable motional heterogeneities. A relatively broad distribution of motional modes was found not only in amorphous phase, where mobile polymer segments in "free" domains coexist with immobilized units in "constrained", or even "extra-constrained" ones, but also in the POSS aggregates and crystallites. The high-quality analysis of segmental dynamics performed by "domain-selective" experiments revealed that differences in motional frequencies are associated with differences in motional amplitudes. In some cases the changes in motional amplitudes were quite pronounced, while the relaxation times were apparently affected only slightly. Comparing thermomechanical properties in a view of the molecular behavior of these systems, we found clear correlations; however, no simple dependence between mechanical properties and a single NMR parameter was found. Every mechanical property probed was found to have its own source on several molecular levels that are mutually interrelated. However this situation can be advantageous for tailoring and tuning of the properties of new types of hierarchical polymer systems. As shown, the advanced techniques of solid-state NMR spectroscopy make it possible to at least partially discover these relations and helps with the design of these polymer materials.

Acknowledgment. The authors thank the Grant Agency of Academy of Sciences of the Czech Republic (Grant IAA40050-0602) for financial support.

Supporting Information Available: Text discussing the theoretical calculation of dipolar spectra simulated for various geometry of small spin clusters and figures showing the resulting spectra. This material is available free of charge via the Internet at http://pubs.acs.org.

References and Notes

(1) Frisch, H. L.; Mark, J. E. *Chem. Mater.* **1996**, *8*, 1735.
(2) Thostenson, E. T.; Ren, Z. F.; Chou, T. W. *Compos. Sci. Technol.* **2001**, *61*, 1899.
(3) Ray, S. S.; Okamoto, M. *Prog. Polym. Sci.* **2003**, *28*, 1539.
(4) Lichtenhan, J. D.; Vu, N. Q.; Carter, J. A.; Gilman, J. W.; Feher, F. J. *Macromolecules* **1993**, *26*, 2141.
(5) Lichtenhan, J. D.; Otonari, Y. A.; Carr, M. J. *Macromolecules* **1995**, *28*, 8435.
(6) Haddad, T. S.; Lichtenhan, J. D. *Macromolecules* **1996**, *29*, 7302.
(7) Tsuchida, A.; Bolln, C.; Sernetz, F. G.; Frey, H.; Mulhaupt, R. *Macromolecules* **1997**, *30*, 2818.
(8) Hsiao, B. S.; Fu, X.; Mather, P. T.; Chaffee, K. P.; Jeon, H.; White, H.; Rafailovich, M.; Lichtenhan, J. D.; Schwab, J. J. *Polym. Mater. Sci. Eng.* **1998**, *79*, 389.
(9) Mather, P. T.; Jeon Hong, A.; Romo-Uribe, A.; Haddad, T. S.; Lichtenhan, J. D. *Macromolecules* **1999**, *32*, 1194.
(10) Bassindale, A. R.; Gentle, T. E. *J. Mater. Chem.* **1993**, *3*, 1319.
(11) Matějka, L.; Strachota, A.; Pleštil, J.; Whelan, P.; Steinhart, M.; Šlouf, M. *Macromolecules* **2004**, *37*, 9449.
(12) Strachota, A.; Kroutilová, I.; Kovářová, J.; Matějka, L. *Macromolecules* **2004**, *37*, 9457.
(13) Lichtenhan, J. D.; Haddad, T. S.; Schwab, J. J.; Carr, M. J.; Chaffee, K. P.; Mather, P. T. *Polym. Prepr.* **1998**, *39* (1), 489.
(14) Zheng, L.; Waddon, A. J.; Farris, R. J.; Farris, R. J.; Coughlin, E. B. *Macromolecules* **2002**, *35*, 2375.
(15) Brown, S. P.; Spiess, H. W. *Chem. Rev.* **2001**, *101*, 4125.
(16) Brus, J.; Dybal, J. *Macromolecules* **2002**, *35*, 10038.
(17) Brus, J.; Petřícková, H.; Dybal, J. *Monatsh. Chem.* **2002**, *133*, 1587.
(18) Brown, S. P. *Prog. Nucl. Magn. Reson. Spectrosc.* **2007**, *50* (4), 199.
(19) Hong, M.; Yao, X. L.; Jakes, K.; Huster, D. *J. Phys. Chem. B* **2002**, *106*, 7355.
(20) Brus, J.; Urbanova, M. *J. Phys. Chem. A* **2005**, *109*, 5050.
(21) Brus, J.; Urbanova, M.; Kelnar, I.; Kotek, J. *Macromolecules* **2006**, *39* (16), 5400.
(22) Hou, S. S.; Bonagamba, T. J.; Beyer, F. L.; Madison, P. H.; Schmidt-Rohr, K. *Macromolecules* **2003**, *36*, 2769.
(23) Yang, D. K.; Zax, D. B. *J. Chem. Phys.* **1999**, *110*, 5325.
(24) Hou, S. S.; Beyer, F. L.; Schmidt-Rohr, K. *Solid State Nucl. Magn. Reson.* **2002**, *22*, 110.
(25) De Paul, S. M.; Zwanziger, J. W.; Ulrich, R..; Wiesner, U.; Spiess, H. W. *J. Am. Chem. Soc.* **1999**, *121*, 5727.
(26) Pawsey, S.; McCormick, M.; De Paul, S.; Graf, R.; Lee, Y. S.; Reven, L.; Spiess, H. W. *J. Am. Chem. Soc.* **2003**, *125*, 4174.
(27) Brus, J.; Dybal, J.; Schmidt, P.; Kratochvíl, P.; Baldrian, J. *Macromolecules* **2000**, *33*, 6448.
(28) Brus, J.; Dybal, J.; Sysel, P.; Hobzová, R. *Macromolecules* **2002**, *35*, 1253.
(29) Brus, J.; Spirkova, M.; Hlavata, D.; Strachota, A. *Macromolecules* **2004**, *37*, 1346.
(30) Torchia, D. A. *J. Magn. Reson.* **1978**, *30*, 613.
(31) Brus, J. *Solid-State Nucl. Magn. Reson.* **2000**, *16*, 151.
(32) van Rossum, B. J.; de Groot, C. P.; Ladizhansky, V.; Vega, S.; de Groot, H. J. M. J. *Am. Chem. Soc.* **2000**, *122*, 3465.
(33) Ladizhansky, V.; Vega, S. *J. Chem. Phys.* **2000**, *112*, 7158.
(34) Lee, M.; Goldburg, W. *Phys. Rev.* **1965**, *140*, A1261.
(35) Wu, C. H.; Ramamoorthy, A.; Opella, S. J. *J. Magn. Reson. Ser A* **1994**, *109*, 270.
(36) Dvinskikh, S. V.; Zimmermann, H.; Maliniak, A.; Sandström, D. *J. Magn. Reson.* **2003**, *164*, 165.
(37) Richter, I.; Burschka, C.; Tacke, R. *J. Org. Chem.* **2002**, *646*, 200.
(38) Bonhomme, C.; Toledano, P.; Maquet, J.; Livage, J.; Bonhomme-Coury, L. *J. Chem. Soc., Dalton Trans.* **1997**, *9*, 1617.
(39) Clauss, J.; Schmidt-Rohr, K.; Spiess, H. W. *Acta Polym.* **1993**, *44*, 1.
(40) Burum, D. P.; Rhim, W. K. *J. Chem. Phys.* **1979**, *71*, 944.
(41) Bielecki, A.; Kolbert, A. C.; de Groot, H. J. M.; Griffin, R. G.; Levitt, M. H. *Adv. Magn. Reson.* **1990**, *14*, 111.
(42) Lesage, A.; Sakellariou, D.; Hediger, S.; Elena, B.; Charmont, P.; Steuernagel, S.; Emsley, L. *J. Magn. Reson.* **2003**, *163*, 105.
(43) Pechar, M.; Brus, J.; Kostka, L.; Konak, C.; Urbanova, M.; Slouf, M. *Macromol. Biosci.* **2007**, *7*, 56.
(44) Schmidt-Rohr, K.; Spiess, H. W. *Multidimensional Solid-State NMR and Polymers*; Academic Press: San Diego, CA, 1994.
(45) Jia, X.; Wolak, J.; Wang, X. W.; White, J. L. *Macromolecules* **2003**, *36*, 712.

(46) Schmidt-Rohr, K.; Clauss, J.; Spiess, H. W. *Macromolecules* **1992**, *25*, 3273.
(47) Mellinger, F.; Wilhelm, M.; Spiess, H. W. *Macromolecules* **1999**, *32*, 4686.
(48) Palmer, A. G.; Williams, J.; McDermott, A. *J. Phys. Chem.* **1996**, *100*, 13293.
(49) Brus, J.; Jakeš, J. *Solid-State Nucl. Magn. Reson.* **2005**, *27*, 180.
(50) Huster, D.; Xiao, L. S.; Hong, M. *Biochemistry* **2001**, *40*, 7662.
(51) Lipari, G.; Szabo, A. *J. Am. Chem. Soc.* **1982**, *104*, 4546.
(52) Brüschweiler, R.; Wright, P. E. *J. Am. Chem. Soc.* **1994**, *116*, 8426.
(53) Zemke, K.; Schmidt-Rohr, K.; Spiess, H. W. *Acta Polym.* **1994**, *45*, 148.
(54) Zucchi, I. A.; Galante, M. J.; Williams, R. J. J.; Franchini, E.; Galy, J.; Gerard, J. F. *Macromolecules* **2007**, *40*, 1274.
(55) Strachota, A.; Whelan, P.; Kriz, J.; Brus, J.; Urbanova, M.; Slouf, M.; Matejka, L. *Polymer* **2007**, *48*, 3041.

MA702140G